

Decision analysis for robust CO₂ injection: Application of Bayesian-Information-Gap Decision Theory



Matthew Grasinger^{a,*}, Daniel O'Malley^b, Velimir Vesselinov^b, Satish Karra^b

^a Civil and Environmental Engineering Department, University of Pittsburgh, United States

^b Computational Earth Science Group, Los Alamos National Laboratory, United States

ARTICLE INFO

Article history:

Received 31 August 2015
Received in revised form 9 February 2016
Accepted 11 February 2016
Available online 3 March 2016

Keywords:

Decision analysis
Decision theory
Bayesian inference
Uncertainty quantification
Multiphase flow
CO₂ sequestration
Site selection

ABSTRACT

Care must be taken when choosing a site for geological CO₂ sequestration to ensure that the CO₂ remains sequestered for many years, and that the environment is not harmed. Making a decision between sites for sequestration is not without its challenges because, as in the case of many subsurface problems, there are a lot of uncertainties. A method for making decisions under various types and severities of uncertainties, Bayesian-Information-Gap Decision Theory (BIG DT), is coupled with a numerical multiphase flow model for CO₂ injection. The framework is used to make a decision between two CO₂ sequestration sites; data are collected during a test injection and are used by the framework to assess the robustness of each site against failure by either leakage or induced seismic activity. A discussion of how the data are used to decide on a site follows. The results show that at the two synthetic sites examined here, the one with the less leakage potential is preferred. This indicates that the potential for leakage is more prone to violate decision goals at these sites than the potential for overpressurization.

© 2016 Elsevier Ltd. All rights reserved.

1. Introduction

Geological carbon sequestration is the act of capturing carbon dioxide from coal and natural gas power plants or industrial processes and storing it deep in underground geologic formations. This approach has the potential to mitigate global climate change by limiting the emission of greenhouse gases into the atmosphere. The U.S. Department of Energy estimates that 1800–20,000 billion tons of CO₂ can be stored below ground in the United States (The North American, 2012). This represents 600–6700 years of carbon dioxide emissions at the current rate of emission.

Despite the potential for geological carbon sequestration to reduce greenhouse gas emissions, there are challenges and potential risks that must be considered when selecting a site for injection. Injecting CO₂ at pressures much higher than natural formation pressures can cause the formations to fracture and slip along faults. Formation fracture and movement can open up leakage pathways for CO₂ to migrate through (Wo and Liang, 2005), or pressure buildup (Zhou et al., 2008; Birkholzer et al., 2009) can cause earthquakes – potentially severe enough to damage to local infrastructure (Healy et al., 1968). CO₂ site selection must be done with

care to reduce the potential for: (1) CO₂ or brine leakage – which can migrate into groundwater or into the atmosphere (in the case of CO₂), and (2) rock formation fracture and slip.

One of the challenges in deciding among various potential sites for geological CO₂ sequestration is the uncertainty in the subsurface. Subsurface conditions can be highly variable, e.g., formation properties such as permeability, porosity, and rock density can vary significantly with short distances or changes in depth and are prohibitively difficult to measure (Blainey, 2008). In addition, the subsurface conditions of the wells constructed at the geological CO₂ sequestration sites are difficult to evaluate and monitor (e.g., well casing integrity and wellbore cementation conditions). Making a rational decision under these circumstances requires quantifying and considering such uncertainties. It is important to note that frequently not all the uncertainties in the subsurface can be characterized probabilistically. Typically, the uncertainty in the subsurface are non-probabilistic (O'Malley and Vesselinov, 2014, 2015).

Recently, the U.S. Department of Energy developed a series of best practice manuals for carbon capture and storage (Rodosta et al., 2011). While best practices can be useful for preliminary analysis or making simple decisions, they often do not generalize well to the complex physics and innumerable uncertainties associated with performing a rigorous analysis of predicting what will occur at a particular CO₂ injection site. Often times, more thorough analyses than what a best practice manual can offer, are performed

* Corresponding author.

E-mail addresses: grasingerm@pitt.edu (M. Grasinger), omalley@lanl.gov (D. O'Malley), vvv@lanl.gov (V. Vesselinov), satkarra@lanl.gov (S. Karra).

by scientists and engineers. Many analytical, semi-analytical, and numerical models have been developed in the past to investigate the complex multiphase reactive transport of CO₂ in the subsurface (Zheng et al., 2013; Nordbotten et al., 2005, 2008; Xiao et al., 2011; Ruan et al., 2013; Schwartz, 2014; Sun et al., 2013).

Forward models with complex processes are only reliable for decision-making on a suitable site for CO₂ injection when the parameters of the sites of interest are known and well-defined. To account for the uncertainty in the subsurface, methods for inverse analysis are needed. Gasda et al. (2011) developed a method to estimate the permeability (leakage) along abandoned wellbores through inverse analysis of measured data. Jung et al. (2012) used pressure anomalies measured from monitoring wells to detect the presence of leakage pathways for CO₂ to escape through. Although Gasda et al. and Jung et al. provided methods for inversely determining the parameters of possible CO₂ sequestration sites, their methods do not represent complete frameworks for decision-making. Wang and Small (2014) used pressure measurements from monitoring wells and Bayesian inference to characterize the reservoir properties and probability of CO₂ leakage. They focused primarily on diffusive leakage and did not consider leakage through high permeability pathways. Wang and Small were able to show the utility of using pressure measurements for Bayesian inference in CO₂ sequestration; however, they did not consider non-probabilistic methods for decision analysis or uncertainty quantification. Non-probabilistic uncertainties can be very important to consider in the decision-making process because, as discussed previously, much of the uncertainty in subsurface problems cannot be characterized probabilistically.

Recently, O'Malley and Vesselinov (2014, 2015) presented a Bayesian-Information-Gap Decision Theory (BIG DT) framework for making decisions under various types and severities of uncertainty. O'Malley and Vesselinov (2015) applied BIG DT to site selection for CO₂ sequestration, however, the physical model that was used in their work was simple and suffered serious limitations in the physics of which it could characterize. The physical model was an analytical model that only considered a single-phase flow of brine and assumed that the aquifers were each homogeneous, isotropic, extended infinitely, and were separated by completely impermeable layers.

In the current work, the limitations of the previous works are addressed by using an alternative numerical method for implementing the BIG DT approach that enables us to utilize a more realistic model with complex physics. BIG DT analysis is performed using the open-source code MADS (Vesselinov et al., 2015) (Model-Analyses & Decision Support). MADS is coupled with the forward physical model used in this work, PFLOTRAN (Lichtner et al., 2015), which can characterize the multicomponent multiphase CO₂-brine flow in the subsurface that occurs during CO₂ injection. As a result, both the Bayesian inference and assessment of whether or not a potential injection well meets the performance goals may be done more accurately.

The outline of the paper is as follows. The forward physical PFLOTRAN model used and the BIG DT approach based on this model are described in Section 2. Analysis of the BIG DT approach coupled to the PFLOTRAN model is performed in Section 3 followed by the conclusion in Section 4.

2. Methods

BIG DT is an approach that uses a combination of observations, forward modeling and Bayesian statistics to infer the probable parameters of a system. Because, as discussed previously, not all of the unknowns present can be characterized probabilistically, another layer in the computational framework is added to

the Bayesian approach in order to quantify these uncertainties non-probabilistically. This additional layer is the Information-gap Decision Theory. The result of combining these approaches is a framework that allows an investigator to make a decision under various types and severities of uncertainty in a rigorous and mathematically justifiable manner.

2.1. Physical model

Geological CO₂ sequestration is a complex physical process, where CO₂ is injected deep into a highly permeable rock formation, at high pressures. Depending on the magnitude of the pressure and temperature, the CO₂ may be in a gaseous phase or a supercritical phase. In order to model CO₂ injection, we used the parallel open-source multiphase flow and reactive transport simulator PFLOTRAN. PFLOTRAN was applied to simulate two-phase flow of brine and CO₂ in the subsurface accounting for complex processes such as: convective instabilities due to dissolution of CO₂ in brine (Lu and Lichtner, 2007), characterizing the geochemical response due to CO₂ leakage (Navarre-Sitchler et al., 2013), and evaluating the potential usage of supercritical CO₂ as a working fluid for enhanced geothermal systems (Lichtner and Karra, 2014). The physical domain considered for our analysis involved a two-dimensional box 500 m × 500 m with 1 m thickness. Details of the governing equations and the implementation of the two-phase brine-CO₂ flow in PFLOTRAN can be found in (Lu and Lichtner, 2007; Lichtner et al., 2015).

The model set-up was as follows. A 100 m thick upper aquifer was confined between two 100 m thick, low permeability caprocks. The bottom 200 m of the domain represented the lower aquifer into which the CO₂ was injected. Hydrostatic boundary conditions were used for the $x=0$ and $x=500$ boundaries, and closed boundary conditions were used at $z=0$ and $z=500$. There were two observation screens, one in the lower aquifer (350, 100) m and one in the upper aquifer (350, 350) m; the observation screens were points in which measurements were taken for the purpose of Bayesian inference. The observations are depicted in Fig. 1. The CO₂ was injected at (250, 100) m in supercritical phase. A 10 m wide leakage path was included in the model. The parameters used in the PFLOTRAN model are summarized in Table 1. A schematic of the domain is shown in Fig. 2. Profiles of pressure change from initial (in orange) along with CO₂ saturation contours (in blue) at 3 different times (1 day, 15 days, and 30 days) is shown in Fig. 3, for one of the two sites that were studied. As CO₂ was injected in the lower aquifer, at initial

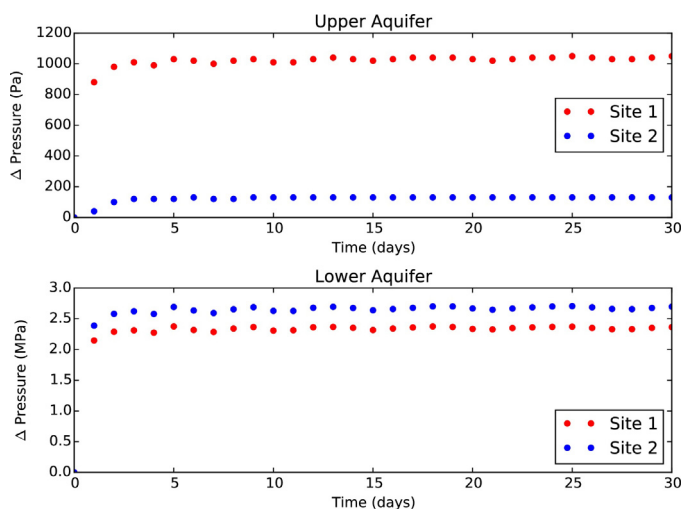


Fig. 1. The change (from initial) in pressure in the upper (top) and lower (bottom) aquifers over the course of a 30 day injection test at each of the two sites.

Table 1
Parameters used in the PFLOTRAN CO₂ injection model.

Property		Value	Units
Domain size,	$x \times z$	500 × 500	(m × m)
Number of grid cells,	$x \times z$	50 × 50	(–)
Lower aquifer,	z-coordinates	0–200	(m)
Lower caprock,	z-coordinates	200–300	(m)
Upper aquifer,	z-coordinates	300–400	(m)
Upper caprock,	z-coordinates	400–500	(m)
Lower observation screen,	(x, z)	(350, 100)	(m)
Upper observation screen,	(x, z)	(350, 350)	(m)
Leakage path,	x-coordinate	400	(m)
Injection point,	(x, z)	(250, 100)	(m)
Injection rate,	–	0.1	(kg/s)
Pressure datum,	(x, z)	(0, 500)	(m)
Initial pressure at datum,	–	20	(MPa)
Initial temperature,	–	50	(°C)
Lower aquifer,	permeability	1×10^{-14}	(m ²)
Lower aquifer,	porosity	0.05	(–)
Lower aquifer,	density	2.65×10^3	(kg/m ³)
Upper aquifer,	permeability	1×10^{-12}	(m ²)
Upper aquifer,	porosity	0.3	(–)
Upper aquifer,	density	1.65×10^3	(kg/m ³)
Caprock aquifer,	permeability	1×10^{-20}	(m ²)
Caprock aquifer,	porosity	0.15	(–)
Caprock aquifer,	density	2.65×10^3	(kg/m ³)
Leaky well, Site 1,	permeability	1×10^{-14}	(m ²)
Leaky well, Site 2,	permeability	1×10^{-15}	(m ²)
Leaky well, Site 1 and 2,	porosity	0.15	(–)
Leaky well, Site 1 and 2,	density	2.65×10^3	(kg/m ³)
Total observation time	–	30	(d)

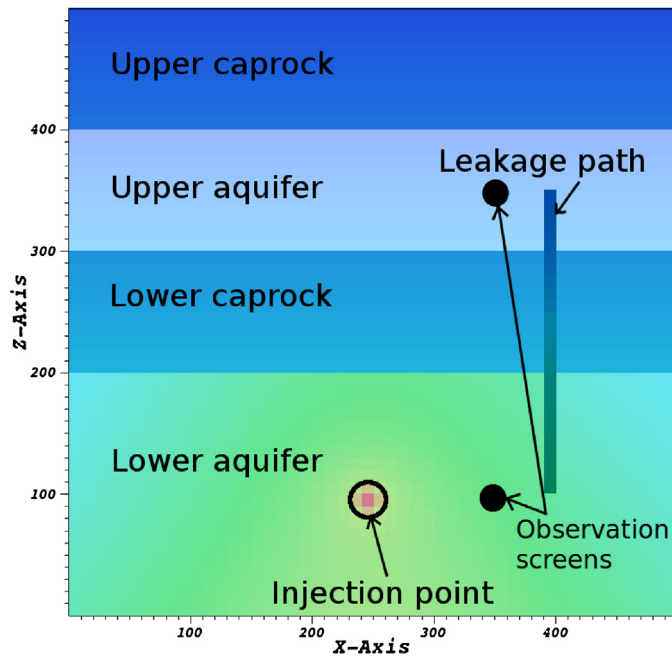


Fig. 2. Model domain and schematic representation of features in the physical PFLOTRAN CO₂ sequestration model. Each region in the domain that represents a new material is a different shade of blue. The second color map, overlaying the regional differences, is of pressure contours. It can be seen that at that particular time step (day 1) the pressure was highest at the injection point (red) and progressively more relaxed as the radial distance from the injection point increased (green). (For interpretation of the references to colour in this figure legend, the reader is referred to the web version of this article.)

times, pressure in the lower aquifer increased. This increase in the pressure pushed the brine in place to the upper aquifer through the leaky well. This migration of brine to the upper aquifer increased the pressure in the upper aquifer. Since the aquifers were assumed to be homogeneous, CO₂ moved radially from the injection point. As Site 1 was more leaky, pressure diffused faster from the lower

to upper aquifer. This can be seen in Fig. 1, where the observation point pressure for Site 1 in the lower aquifer was lower than that of Site 2. Additionally, the observation point pressure in the upper aquifer for Site 1 was higher than Site 2, indicating faster pressure diffusion and more brine migration to the upper aquifer for Site 1 than Site 2.

2.2. Bayesian approach

Bayes' rule is a means for inverting probabilities. When considering a stochastic system, one often inputs parameters and considers a possible set of outcomes (or stochastic events), each with an associated probability often defined according a distribution – this is the forward way of thinking about stochastic systems. Bayesian statistics allows one to invert this probability and instead assess the probability of a parameter set given an outcome, or a stochastic event that has occurred. In other words, Bayesian statistics allows one to use measured data, or observations of the system output, to make an inference about the parameters of the system. In the BIG DT approach, Bayesian statistics are used to address parametric uncertainty. This is important because, as discussed previously, subsurface conditions are variable and difficult to measure.

Bayes' rule is defined mathematically as,

$$f(\mathbf{q}|\mathbf{O}) = \frac{f(\mathbf{O}|\mathbf{q})f(\mathbf{q})}{\int_{\Omega} f(\mathbf{O}|\mathbf{q})f(\mathbf{q})d(\mathbf{q})} \quad (2.1)$$

where \mathbf{q} are the parameters, \mathbf{O} are observations and represent an outcome or event of the system, $f(\mathbf{q})$ is known as the prior distribution, and $f(\mathbf{O}|\mathbf{q})$ is the likelihood function. The prior distribution should contain one's belief about how the parameters of the system are distributed prior to collecting any evidence. The prior distribution allows one to “encode” information about the distribution of parameters that is known before observations are collected. The conditional likelihood function is a function that describes how the observations are distributed given parameters, \mathbf{q} . The conditional likelihood function is generally related to the residuals between observed data and the output of a parametric model of the system (O'Malley and Vesselinov, 2015), i.e.,

$$f(\mathbf{O}|\mathbf{q}) = g(O_1 - F_1(\mathbf{q}), O_2 - F_2(\mathbf{q}), \dots, O_N - F_N(\mathbf{q})) \quad (2.2)$$

where g is some multivariate probability density function, F_j is a model output that corresponds to observation O_j , and $O_j - F_j(\mathbf{q})$ are the residuals.

In practice, the integral in Eq. (2.1) is difficult to compute analytically because the exact form of the model function may be complex and unknown, e.g., in the case of a numerical model, and additionally, the integral is taken over the entire parameter space, which may be a high dimensional space. Monte Carlo methods can instead be used to approximate a solution to Eq. (2.1). In the present work, the Monte Carlo method was used with Latin hypercube sampling (LHS) (Ye, 1998). Note that O'Malley and Vesselinov (2015) had used the Markov chain Monte Carlo (MCMC) approach in their work with the BIG DT approach. We used the Monte Carlo method with LHS since the PFLOTRAN numerical model is computationally expensive and Monte Carlo with LHS allows one to run multiple realizations on a cluster or a supercomputer in an inherently parallel fashion as opposed to MCMC which runs a chain of simulations. LHS was used, as opposed to random sampling, to ensure that the ensemble of parameter samples were representative of a “true” variability, and the samples were not biased toward any specific region of the parameter space. Some statistics of the random sampling are presented in Fig. 4.

For the Bayesian approach used in the present work the parameter space was two-dimensional. The parameter vector is defined

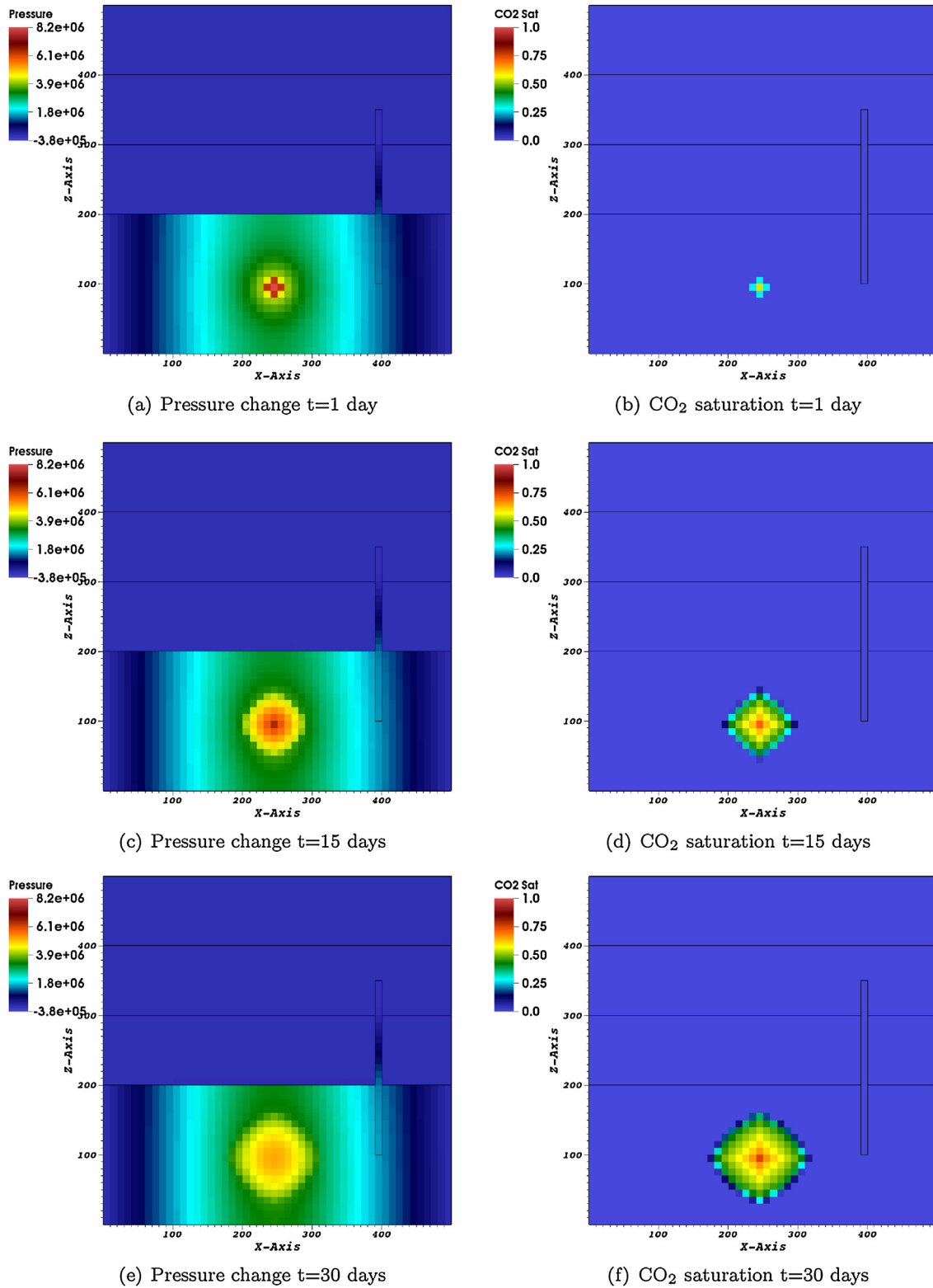


Fig. 3. Profiles of pressure change from initial pressure (left set of figures) and CO₂ saturation (right set of figures) for the more leaky Site 1 case. The Pressure legend shown is in Pa.

as, $\mathbf{q} = [R, \log(k)]$, where R is the location (x -coordinate) of the leakage path, and $\log(k)$ is the logarithm of the permeability along the leakage pathway. The parametric uncertainty considered was the location of a leakage pathway and its potential for leakage, all other parameters were assumed to be known. The parameters can be seen in Table 1.

The prior likelihood function used in the present work is defined as follows:

$$f(\mathbf{q}) = f_1(R)f_2(\log(k)) \quad (2.3)$$

where $f_1(x)$ is a uniform likelihood function on the intervals $[0, 225]$ and $[275, 500]$, i.e., any location at a distance of greater than or

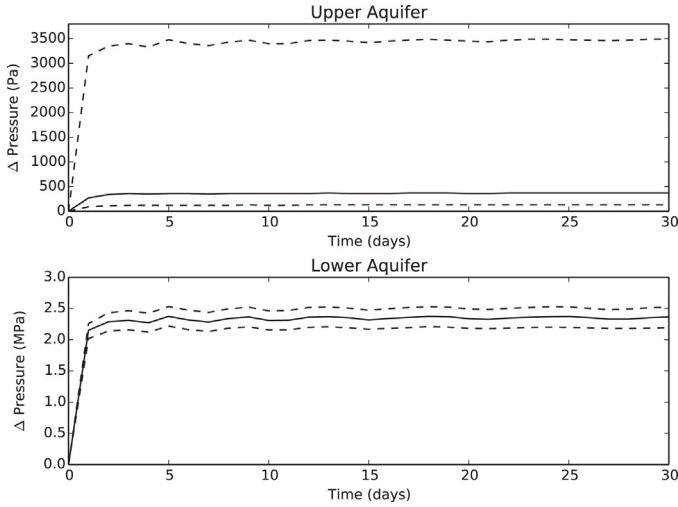


Fig. 4. The solid line shows the median change in pressure induced by the injection during the Monte Carlo simulations. The two dotted lines show the 25th and 75th percentiles.

Table 2
Bounds in parametric uncertainty.

Parameter	Bounds
R	[0, 225], [275, 450] (m)
log(k)	[-16, -12] (m ²)

equal to 25 m from the point of injection, and $f_2(x)$ is a uniform likelihood function on the interval $[-16, -12]$ where k is in m². The uncertainty bounds are summarized in Table 2.

The conditional likelihood function used was a multivariate, zero mean Gaussian distribution with a covariance matrix defined as:

$$\Sigma_{ij} = \frac{\sigma^2}{2} (|t_i + 1 - t_j|^{2H} - 2|t_i - t_j|^{2H} + |t_i - 1 - t_j|^{2H}) \quad (2.4)$$

where $\sigma = 2.5$ cm is the standard deviation, t_i is the time at the i th observation, and H is the Hurst exponent. Eq. (2.4) is the covariance for a signal with fractional Gaussian noise. When $H = 1/2$, the noise is a Gaussian white noise which exhibits neither persistence nor anti-persistence. Gaussian white noise is the expected noise if the residuals are unbiased, independent, and normally distributed (O'Malley and Vesselinov, 2015).

2.3. Information-Gap Decision Theory

Information-Gap Decision Theory (IGDT) is a non-probabilistic method for quantifying uncertainty, and in particular, for answering the question: "How wrong can our best guess be before the possibility for failure exists?" Because IGDT is non-probabilistic, it does not consider the frequency, or probability of events, but instead it focuses only on 'clustering' sets of events (Ben-Haim, 2006). Although neglecting probability may seem like a disadvantage for a decision theory at first glance, and that information may be left out in the process, there are strategic reasons why, in some instances, neglecting probability is advantageous:

1. There are certain instances in which uncertainty cannot be addressed by parameterizing and assigning a probability to all possibilities, e.g., it would not be practical to try to consider the set of all possible physical models and assign a probability to each. For this reason, one of the uncertainties addressed by IGDT

in the current work was uncertainty in the model (i.e., conceptual and model-representation uncertainties).

2. If the actual distribution that governs a phenomena is unknown, which is often the case, then guessing one, even if it is approximately correct, can have consequences. In this case, the probabilistic model is imposing information into the decision process that is unknown and possibly untrue. A consequence that can occur from guessing at a distribution is that the tails of the model may differ substantially from the actual distribution (Ben-Haim, 2006). Events that are represented by the tails of the distribution may be exactly what a decision maker is interested in, because these events typically represent extreme events, and therefore may be a disaster that a decision maker is trying to avoid. IGDT is useful in situations where the actual distribution is unknown because it is not limited by the assumptions or tails of a probability distribution.

Formally, one of the info-gap models used in the current work is expressed as,

$$M(\epsilon, \mathbf{q}) = \left\{ \mathbf{F} : \left| \frac{F_i - F_i(\mathbf{q})}{F_i(\mathbf{q})} \right| \leq \epsilon, i = 1, 2, \dots, N \right\} \quad (2.5)$$

$M(\epsilon, \mathbf{q})$ represents a set of possible outcomes from given parameters \mathbf{q} , within a horizon of uncertainty ϵ . We note that we have represented the model uncertainty here nonparametrically. This is important, because studies have shown that non-parametric model uncertainty can be significantly larger than parametric uncertainty (Ye et al., 2010). These outcomes are all possible model outputs that lie within a relative error of the nominal model $F_i(\mathbf{q})$, or expressed differently, all possible model outputs for which the relative infinity norm between the possible model output and nominal model output, is less than or equal to a chosen horizon of uncertainty. The nominal model is the term used to identify the best guess for a particular phenomena. In the case of CO₂ injection, the nominal model will be the direct output of the PFLOTTRAN physical model. A geometric interpretation of this set would be, if the output of the model were in a two-dimensional space (F_1, F_2), a square with side length 2ϵ and centered at the nominal model ($F_1(\mathbf{q}), F_2(\mathbf{q})$). Note that, at a horizon of uncertainty of zero, BIG DT is equivalent to a purely Bayesian approach.

Since the aim of IGDT is to answer the question: "How wrong can our best guess be before the possibility for failure exists?", in terms of the info-gap model defined in Eq. (2.5), this question can be answered mathematically as the largest set (or correspondingly, largest horizon of uncertainty) of possible outcomes for which none of the outcomes within the set represent failure. The largest horizon of uncertainty for which failure is not in the set of possibilities will be defined as the robustness of the decision (Ben-Haim, 2006). IGDT allows one to measure the most robust decision against failure. In the case of the present work, the interest was in the potential site for CO₂ sequestration that was most robust against failure. In order to calculate robustness, one must first define what constitutes failure. The criteria that define whether or not failure has occurred will be referred to as performance goals.

There are criteria that a decision maker would attempt to meet when choosing a site for CO₂ sequestration:

1. Choose a site that is robust against leakage of brine or CO₂ out of the lower formation. This is necessary to protect groundwater and the atmosphere.
2. Choose a site that is robust against induced seismicity as a result of the injection.

With these criteria in mind, two performance goals that have been used in the current work to define failure, and are expressed mathematically as:

$$\begin{cases} \Delta h_1 \leq 2500 \text{ Pa}, \\ \Delta h_2 \leq 10 \text{ MPa} \end{cases} \quad (2.6)$$

where Δh_1 is the maximum increase in head in the upper aquifer over the injection period, and Δh_2 is the maximum increase in head in the lower aquifer over the injection period. An increase in head in the upper aquifer Δh_1 , that is greater than or equal to 2500 Pa, is a threshold that is being used as an early indicator the potential for injection in the lower aquifer to cause the upper aquifer to become contaminated with fluid from the lower aquifer (brine or CO₂). An increase in head in the lower aquifer Δh_2 , that is greater than or equal to 10 MPa, indicates a significant increase in pressure that could potentially cause a seismic event. The robustness of a potential CO₂ injection site is measured by the largest horizon of uncertainty for which none of the possible outcomes within the set defined by the horizon of uncertainty fail either of the performance goals.

These decision goals expressed in Eq. (2.6) are subject to revision depending on the goals of the decision-maker. Here, we consider a short-term pump test (30 days) to evaluate the robustness of the sites. On a longer time scale, it would be appropriate to include a performance requirement that limits the amount of CO₂ that is detected in the upper aquifer. On the 30 day time scale, we have elected to use pressure increases in both the lower and upper aquifers as our performance goals because the pressure propagates much faster than mass is transported – no CO₂ reaches the observation screen in the upper aquifer during the 30 day test. We emphasize again, that the performance goals in Eq. (2.6) are subject to the whim of the decision-maker. The framework we use here can be applied the performance goals in Eq. (2.6) or other performance goals as the decision-maker sees fit.

2.4. Bayesian-Information-Gap Decision Theory

BIG DT is the confluence of two methods – Bayesian as well as IGDT – for addressing uncertainty with the aim of combining the strengths of each. Bayesian statistics are used to address the parametric uncertainty of the physical system. If the probability distribution of the observation errors was known and the physical model was perfectly accurate, the Bayesian approach would suffice at addressing all potential uncertainties. However, this is not the case. IGDT is used to address uncertainty that the Bayesian approach is not always well suited to address, namely: uncertainty in the physical model and uncertainty in the conditional likelihood function for the Bayesian approach (which describes the inaccuracy of the model and the observations). Uncertainty in the conditional likelihood is expressed as

$$U(\epsilon) = \left\{ f_H(\mathbf{O}|\mathbf{q}) : \left| \frac{H - H_0}{H_0} \right| \leq \epsilon, H \in [0.2, 0.8] \right\} \quad (2.7)$$

where $H_0 = 1/2$ and $f_H(\mathbf{O}|\mathbf{q})$ is a multivariate Gaussian likelihood with covariance given in Eq. (2.4) and zero mean. Note that in another study, a different info-gap model of the conditional likelihood could be used capture uncertainty in this function. Here, we have used the parameter H to describe uncertainty in conditional likelihood. In the info-gap uncertainty models (Eqs. (2.5) and (2.7)), the index ϵ is used to describe a set of events that are possible within that horizon of uncertainty.

The algorithm for the present work consists of performing a field test injection for 30 days at two potential sites for CO₂ sequestration and then using BIG DT to measure the robustness of each site against failure. An overview of the algorithm is as follows:

1. Perform test injection at the potential site. Collect pressure data at the observation screens for 30 days.
2. Sample the model parameter space 50,000 times using Latin hypercube sampling within predefined uncertainty bounds (see Table 2).
3. Sample the likelihood parameter space (i.e., sample H) 25 times using Latin hypercube sampling within predefined uncertainty bounds (see Eq. (2.7)).
4. For each conditional likelihood function, i.e., for each value of H :
 - (a) For each parameter sample, \mathbf{q} :
 - i. Predict pressure response of the system using the physics model.
 - ii. Determine the posterior likelihood $f_H(\mathbf{q}|\mathbf{O}) \propto f_H(\mathbf{O}|\mathbf{q})f(\mathbf{q})$ using Eq. (2.1).
 - (b) For each horizon of uncertainty, ϵ :
 - i. Use the posterior likelihoods from 4.a.ii to determine the probability that $M(\epsilon, \mathbf{q})$ contains an outcome that does not satisfy the performance goals in Eq. (2.6). For a particular ϵ and \mathbf{q} , the performance goals fail if $\Delta h_1(\mathbf{q}) > 2500/(1 + \epsilon)$ Pa or $\Delta h_2(\mathbf{q}) > 10/(1 + \epsilon)$ MPa. The probability that $M(\epsilon, \mathbf{q})$ contains an outcome that does not satisfy the performance goals is obtained by summing over the values of \mathbf{q} .
 - ii. If $\left| \frac{H - H_0}{H_0} \right| \leq \epsilon$ and the probability computed in 4.b.i is greater than the maximum probability seen so far for the chosen horizon of uncertainty ϵ , then increase the maximum probability for the chosen ϵ to the value computed in 4.b.i.
5. Using the maximum probability obtained in Step 4 for each ϵ , generate the robustness curve.

3. Results and discussion

The BIG DT framework for decision analysis and uncertainty quantification that is presented in this work was applied to make a selection between two potential sites for CO₂ injection. Both sites were consistent with the schematic pictured in Fig. 2 and the leakage pathway in both sites was located at $x = 400$ m. The ‘true’ permeability of the leakage path was 10^{-14} for Site 1 and 10^{-15} for Site 2. For the example presented, in lieu of actual measured observations, observations were generated by modeling each site with PFLOTRAN using the true parameters, and then adding random noise using the covariance matrix defined in Eq. (2.4) with a Hurst exponent, $H = 3/4$. The noise was added in order to simulate the noise that would occur in actual collected data. The algorithm described in Section 2.4 was then used to generate robustness curves for each site. The robustness curves for both the sites are compared in Fig. 5. In Fig. 5, as the horizon of uncertainty, ϵ , increases from 0 to 0.6 a larger set of possible likelihoods (Eq. (2.7)) and models (Eq. (2.5)) are being considered, thereby producing a greater “maximum probability of failure”. Once ϵ reaches 0.6, all values of H in the range $[0.2, 0.8]$ are possible. As ϵ increases from 0.6 upward, the increasing “maximum probability of failure” is due entirely to model uncertainty (Eq. (2.5)).

Due to the intersection of the two robustness curves at horizon of uncertainty $\epsilon \approx 2.7$, Fig. 5 can be divided into two separate sections. For the first section ($\epsilon < 2.7$), Site 2 has a lower maximum probability of failure and would be the site one would choose if they considered the first section only. In the first section, outcomes of failure were predominantly a result of not meeting the first performance goal, or the failure that CO₂ had leaked from the lower aquifer up into the upper aquifer. The decision result in the first section is consistent with intuition, as one would expect the site with a leakier leakage path to fail the first performance goal, $\Delta h_1 \leq 2500$ Pa. However, at horizon of uncertainty $\epsilon \approx 2.3$, there is a sharp increase in maximum probability of failure for Site 2

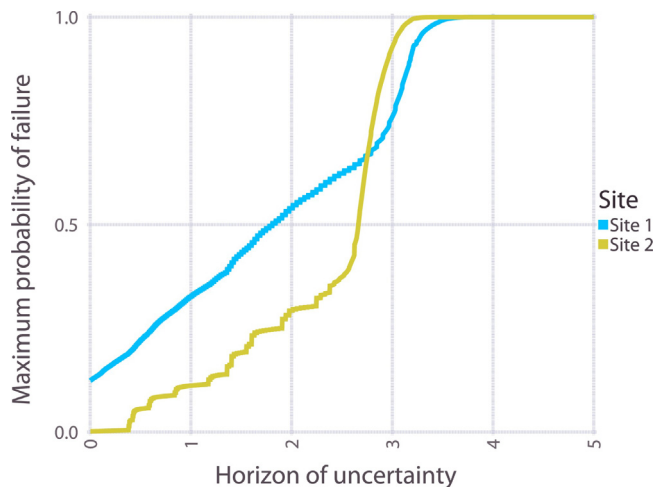


Fig. 5. Robustness curves for Site 1 and Site 2. For $\epsilon < 2.7$ failure is governed by the first performance goal, $\Delta h_1 \leq 2500$ Pa, and represents CO₂ leaking into the upper aquifer. For $\epsilon \geq 2.7$ failure is governed by the second performance goal, $\Delta h_2 \leq 10$ MPa, and represents induced seismic activity.

(and shortly after, Site 1 as well). As a result, for the second section ($\epsilon > 2.7$), Site 1 has a lower maximum probability of failure for a given horizon of uncertainty and would be the site one would choose if they had considered the second section. In the second section of the plot, failure is mostly determined by the second performance goal, $\Delta h_2 \leq 10$ MPa. Again this is consistent with intuition as one would expect the site with a less leaky leakage path to build up more pressure in the lower aquifer as a result of having less of an avenue for the release of that pressure.

At first glance, the more robust site for CO₂ sequestration may seem ambiguous as it depends on which section of the curve one considers to be more important. However, when making a decision in BIG DT, one does not consider “sections” of the robustness curves, but instead makes a decision by deciding on a maximum acceptable probability of failure. Typical values of maximum acceptable probabilities of failure are 5% and below. In this case, Site 2 would be the more robust choice.

4. Conclusion

Bayesian-Information-Gap Decision Theory is a decision framework combining both probabilistic and non-probabilistic methods for dealing with uncertainty. BIG DT was presented and shown to be a method capable of considering different types of uncertainty and making a mathematically robust decision. BIG DT was then applied to the problem of deciding between two potential sites for CO₂ sequestration. The BIG DT is a general framework and is capable of performing decision analysis in any scenario in which parametric, model, and measurement uncertainties exist, making it well-suited for many environmental and subsurface problems.

Acknowledgments

The authors acknowledge the support for this research from the Mickey Leland Energy Fellowship program and the U.S. Department of Energy. DO was supported by a Los Alamos National Laboratory (LANL) Director’s Postdoctoral Fellowship, VVV was supported by the DiaMonD project (An Integrated Multifaceted Approach to Mathematics at the Interfaces of Data, Models, and Decisions, U.S. Department of Energy Office of Science, Grant #11145687), and SK was supported by LANL Laboratory Directed Research and

Development Early Career project 20150693ECR during the preparation of this manuscript.

References

2012. The North American Carbon Storage Atlas, 1st ed. <http://www.netl.doe.gov/File%20Library/Research/Carbon-Storage/NACSA2012.pdf>.
- Ben-Haim, Y., 2006. *Info-gap Decision Theory: Decisions Under Severe Uncertainty*. Academic Press, Oxford.
- Birkholzer, J.T., Zhou, Q., Tsang, C.-F., 2009. Large-scale impact of CO₂ storage in deep saline aquifers: a sensitivity study on pressure response in stratified systems. *Int. J. Greenh. Gas Control* 3 (2), 181–194. <http://dx.doi.org/10.1016/j.ijggc.2008.08.002>.
- Blainey, J.B., 2008. *Using Coupled Modeling Approaches To Quantify Hydrologic Prediction Uncertainty and to Design Effective Monitoring Networks*. University of Arizona.
- Gasda, S.E., Wang, J.Z., Celia, M.A., 2011. Analysis of in-situ wellbore integrity data for existing wells with long-term exposure to CO₂. *Energy Procedia* 4, 5406–5413.
- Healy, J.H., Rubey, W.W., Griggs, D.T., Raleigh, C.B., 1968. The Denver earthquakes. *Science* 161 (3848), 1301–1310.
- Jung, Y., Zhou, Q., Birkholzer, J.T., 2012. Impact of data uncertainty on identifying leakage pathways in CO₂ geologic storage systems and estimating their hydrogeological properties by inverse modeling. In: *TOUGH Symposium*, Berkeley, CA. Lawrence Berkeley National Laboratory.
- Lichtner, P., Hammond, G., Lu, C., Karra, S., Bisht, G., Andre, B., Mills, R., Kumar, J., 2015. *PFLOTRAN user manual: a massively parallel reactive flow and transport model for describing surface and subsurface processes*. Technical Report No.: LA-UR-15-20403. Los Alamos National Laboratory.
- Lichtner, P.C., Karra, S., 2014. Modeling multiscale-multiphase-multicomponent reactive flows in porous media: application to CO₂ sequestration and enhanced geothermal energy using PFLOTRAN. In: Al-Khoury, R., Bundschuh, J. (Eds.), *Computational Models for CO₂ Geo-sequestration & Compressed Air Energy Storage*. CRC Press, pp. 81–136. <http://www.crcnetbase.com/doi/pdfplus/10.1201/b16790-6>.
- Lu, C., Lichtner, P.C., 2007. High resolution numerical investigation on the effect of convective instability on long term CO₂ storage in saline aquifers. In: *Journal of Physics: Conference Series*, vol. 78. IOP Publishing, p. 012042.
- Navarre-Sitchler, A.K., Maxwell, R.M., Siirila, E.R., Hammond, G.E., Lichtner, P.C., 2013. Elucidating geochemical response of shallow heterogeneous aquifers to CO₂ leakage using high-performance computing: implications for monitoring of CO₂ sequestration. *Adv. Water Resour.* 53, 45–55. <http://dx.doi.org/10.1016/j.advwatres.2012.10.005>, ISSN 0309-1708. <http://www.sciencedirect.com/science/article/pii/S0309170812002679>.
- Nordbotten, J.M., Celia, M.A., Bachu, S., Dahle, H.K., 2005. Semianalytical solution for CO₂ leakage through an abandoned well. *Environ. Sci. Technol.* 39 (2), 602–611.
- Nordbotten, J.M., Kavetski, D., Celia, M.A., Bachu, S., 2008. Model for CO₂ leakage including multiple geological layers and multiple leaky wells. *Environ. Sci. Technol.* 43 (3), 743–749.
- O’Malley, D., Vesselinov, V.V., 2014. A combined probabilistic/nonprobabilistic decision analysis for contaminant remediation. *SIAM/ASA J. Uncertain. Quantif.* 2 (1), 607–621.
- O’Malley, D., Vesselinov, V.V., 2015. Bayesian-information-gap decision theory with an application to CO₂ sequestration. *Water Resour. Res.*, <http://dx.doi.org/10.1002/2015WR017413>, ISSN 1944-7973.
- Rodosta, T.D., Litynski, J.T., Plasynski, S.I., Hickman, S., Frailey, S., Myer, L., 2011. US Department of Energy’s site screening, site selection, and initial characterization for storage of CO₂ in deep geological formations. *Energy Procedia* 4, 4664–4671.
- Ruan, B., Xu, R., Wei, L., Ouyang, X., Luo, F., Jiang, P., 2013. Flow and thermal modeling of CO₂ in injection well during geological sequestration. *Int. J. Greenh. Gas Control* 19, 271–280.
- Schwartz, M.O., 2014. Modelling leakage and groundwater pollution in a hypothetical CO₂ sequestration project. *Int. J. Greenh. Gas Control* 23, 72–85.
- Sun, H., Yao, J., Hua Gao, S., Yan Fan, D., Chen Wang, C., Xue Sun, Z., 2013. Numerical study of CO₂ enhanced natural gas recovery and sequestration in shale gas reservoirs. *Int. J. Greenh. Gas Control* 19, 406–419. <http://dx.doi.org/10.1016/j.ijggc.2013.09.011>, ISSN 1750-5836. <http://www.sciencedirect.com/science/article/pii/S1750583613003447>.
- Vesselinov, V.V., O’Malley, D., et al., 2015. Model analysis and decision support (MADS). <http://mads.lanl.gov>.
- Wang, Z., Small, M.J., 2014. A Bayesian approach to CO₂ leakage detection at saline sequestration sites using pressure measurements. *Int. J. Greenh. Gas Control* 30, 188–196.
- Wo, S., Liang, J.-T., 2005. CO₂ storage in coalbeds: CO₂/N₂ injection and outcrop seepage modeling. In: Thomas, D.C. (Ed.), *Carbon Dioxide Capture for Storage in Deep Geologic Formations*. Elsevier Science, Amsterdam, pp. 827–924. <http://dx.doi.org/10.1016/B978-008044570-0/50141-0>, ISBN 978-0-08-044570-0. <http://www.sciencedirect.com/science/article/pii/B9780080445700501410>.
- Xiao, Y., Macleod, G., Advocate, D.M., Reaves, C., Pottorf, R.J., 2011. Natural CO₂ occurrence in geological formations and the implications on CO₂ storage capacity and site selection. *Energy Procedia* 4, 4688–4695.
- Ye, K.Q., 1998. Orthogonal column Latin hypercubes and their application in computer experiments. *J. Am. Stat. Assoc.* 93 (444), 1430–1439.

- Ye, M., Pohlmann, K.F., Chapman, J.B., Pohl, G.M., Reeves, D.M., 2010. A model-averaging method for assessing groundwater conceptual model uncertainty. *Groundwater* 48 (5), 716–728, <http://dx.doi.org/10.1111/j.1745-6584.2009.00633.x>.
- Zheng, L., Spycher, N., Birkholzer, J., Xu, T., Apps, J., Kharaka, Y., 2013. On modeling the potential impacts of CO₂ sequestration on shallow groundwater: transport of organics and co-injected H₂S by supercritical CO₂ to shallow aquifers. *Int. J. Greenh. Gas Control* 14, 113–127.
- Zhou, Q., Birkholzer, J.T., Tsang, C.-F., Rutqvist, J., 2008. A method for quick assessment of CO₂ storage capacity in closed and semi-closed saline formations. *Int. J. Greenh. Gas Control* 2 (4), 626–639, <http://dx.doi.org/10.1016/j.ijggc.2008.02.004>.